Effects of Media Non-Uniformity on Electrostatic Transfer in Electrophotography

Inan Chen and Ming-Kai Tse; Quality Engineering Associates (QEA), Inc.; Burlington, MA, USA

Abstract

The effects of spatial non-uniformity in material parameters on the electrostatic transfer of toners from photoreceptors to receiving media are investigated with the charge transport model of dielectric relaxation in the receiver. The parameters considered include intrinsic charge density, charge mobility, charge injection strength and permittivity of the receiving media. The detrimental effects are found to be more severe when (1) the spatial period of non-uniformity is large, and/or (2) the transfer time is short. An experimental technique for the determination of such spatial non-uniformity is demonstrated.

Introduction

The quality of electrophotographic images depends on the interplay of process and material involved in each step of the image formation. One of these steps is the transfer of toners on the photoreceptor to intermediate and/or final receiving media, with electrostatic forces. The process requires efficient dielectric relaxation of the media to shift most of the applied bias voltage to the toner layer.[1] Due to the semi-insulating and non-Ohmic nature of the media, it has been suggested that the analysis of this dielectric relaxation by the traditional RC equivalent circuit equation is not adequate.[2,3] Instead, a first principle charge transport model of dielectric relaxation has been formulated to investigate the process.[4] These studies have identified the intrinsic charge density q_i, the charge mobility μ, and the charge injection strength s in the media as the key parameters controlling the transfer force.

In the previous analyses,[2,3] the media were assumed to be homogeneous, having uniform values of these parameters. The analyses were formulated in the form of one-dimensional layer model. The present work extends the investigation to consider the effects of spatial (lateral) non-uniformity of these material parameters on the transfer force and hence, on the image quality.[5]

The charge transport model of dielectric relaxation for two-dimensional analyses is described in the next section. This is followed by the presentation and discussion of numerical results. Examples of spatial non-uniformity measured with the technique[6] introduced earlier are shown in the final section.

Charge Transport Model

The transfer nip is represented by a three-layer configuration consisting of the grounded photoreceptor (PR), the toner layer and the receiver as shown in Fig. 1. A small air gap that may exist between the toner layer and the receiver makes no difference of physical significance in this discussion.

It is assumed that the PR in the dark and the toner layer are insulators with no mobile charges. But the toner layer has a constant and uniform volume charge density q_t. The receiver is a semi-insulator that has mobile positive and negative charges with volume densities $q_p(x, y, t)$ and $q_n(x, y, t)$, respectively, which vary with position and time t.
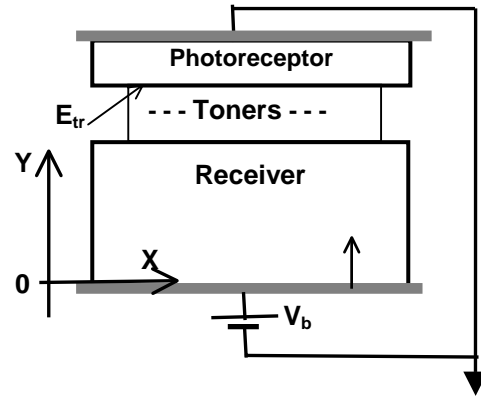

Figure 1. *Three-layer model of transfer nip*

After the bias V_b is applied, the voltages V_k over the layers k (with k = p, t, r for PR, toner and receiver, respectively) change with time due to dielectric relaxation in the receiver. In this analysis, the dielectric relaxation is treated by the charge transport model, as briefly described below.[4]

The continuity equations for conduction currents are used to determine the time and spatial variations of charge densities,

$$\partial q_p/\partial t = -div(\mathbf{J}_p), \quad \partial q_n/\partial t = -div(\mathbf{J}_n) \tag{1}$$

where $\mathbf{J}_p = \mu q_p\mathbf{E}$ and $\mathbf{J}_n = \mu q_n\mathbf{E}$ are the positive and negative conduction currents. The field $\mathbf{E}$ is related to the total space charge density Σq and the permittivity ε by the Poisson equation,

$$div(\mathbf{E}) = (\Sigma q)/\varepsilon \tag{2}$$

Mobile charges are also supplied by injection from the electrode at y = 0. The injection current J_{inj} (in the y-direction) is assumed to be proportional to the y-component of field at the electrode $E_y(x, 0)$, with the proportionality constant s, specifying the injection strength.

$$J_{inj}(x) = J_p(x, 0) = s(x)E_y(x) \tag{3}$$

Starting with the electrostatic initial conditions and the boundary conditions,[3] an iterative numerical procedure for the continuity equations is used to calculate the time evolution of charge densities and the fields. The y component of field in the toner layer at the toner/PR interface is denoted as the transfer field E_{tr}.

The charge transport in the receiver is characterized by the material parameters, including the density of intrinsic mobile charges q_i, the charge mobility μ, the injection strength s, and permittivity ε. Numerical examples of the growth of transfer fields with time, for the cases in which these parameters have uniform values within the layer are shown in Refs. 2 and 3. In the present work, the effects of non-uniformity in these parameters on E_{tr} are considered. The non-uniformity is represented by sinusoidal spatial variations in the lateral (x) direction, i.e.,

$$q_i(x) = q_0 + q_1 cos(\pi x/w) \tag{4A}$$

$$s(x) = s_0 + s_1 cos(\pi x/w) \tag{4B}$$

$$\mu(x) = \mu_0 + \mu_1 cos(\pi x/w) \tag{4C}$$

$$\varepsilon(x) = \varepsilon_0 + \varepsilon_1 cos(\pi x/w) \tag{4D}$$

where w is the half-period of the spatial non-uniformity.

Numerical results are generated for eight cases tabulated in Table I. For clarity in revealing the effects, in each case only one of the parameters is assumed to have the sinusoidal variation (denoted as "*cos*" in the table) while the others have uniform values (1 or 0 in normalized units of Table II).

Table I.

Case	qi	s	μ	ε
A1	*cos*	1	1	1
A2	*cos*	0	1	1
B1	0	*cos*	1	1
B2	1	*cos*	1	1
C1	0	1	*cos*	1
C2	1	0	*cos*	1
D1	0	1	1	*cos*
D2	1	0	1	*cos*

Results and Discussion

The numerical examples are presented in normalized units listed in Table II. The first four basic units are used to define the next five derived ones. The typical values of the units for the present application are also listed for references.

Table II. Normalized Units

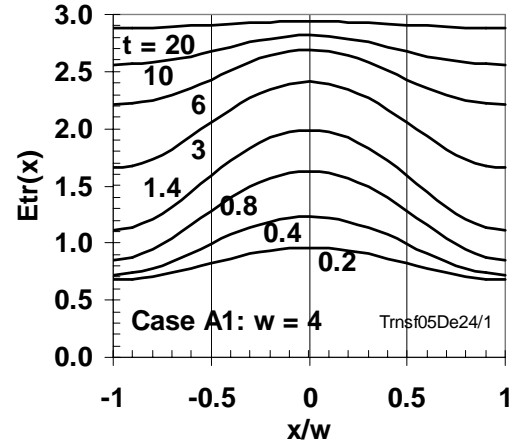| Units	Typical Values
Length: L_r	10^{-2} cm
Permittivity: ε_r	3×10^{-13} F/cm
Voltage: V_b	10^3 V
Charge mobility: μ_o	10^{-5} cm^2/Vsec
- -	
Field: $E_o = V_b/L_r$	10^5 V/cm
Time: $t_o = L_r/\mu_o E_o = L_r^2/\mu_o V_b$	10^{-2} sec
Capacitance: $C_o = \varepsilon_r/L_r$	3×10^{-11} F/cm^2
Charge density (area): $Q_o = C_o V_b$	3×10^{-8} Coul/cm^2
Charge density (vol.): $q_o = Q_o/L_r$	3×10^{-6} Coul/cm^3
Injection strength: $\sigma_o = \mu_o q_o$	3×10^{-11} S/cm

Figure 2. Transfer field E_{tr} distribution due to spatial variation in q_i (Case A1), for w = 4, at different transfer times
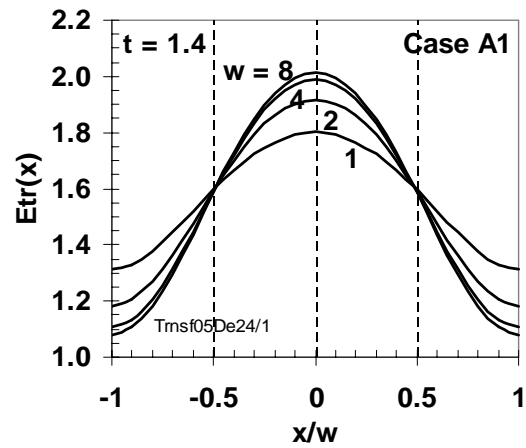

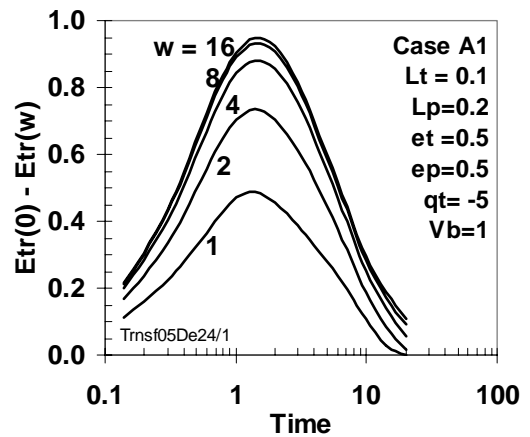**Figure. 3.** E_{tr} distribution for Case A1, for various half-period w.

Figure 2 shows the distribution of $E_{tr}(x)$ over a period (from $x = -w$ to w) due to spatial variation in q_i (case A1), with $w = 4$ (in units of L_r), at different transfer times. The other parameter values are chosen as: layer thickness: $L_r = 1$, $L_t = 0.1$, $L_p = 0.2$; the permittivity: $\varepsilon_r = 1$, $\varepsilon_t = 0.5$, $\varepsilon_p = 0.5$; toner charge density: $q_t = -5$ and bias voltage $V_b = 1$ (all in normalized units of Table II). However, the conclusions are independent of the choice of these parameter values within the range of practical interest. It can be seen that the size of E_{tr} (at any x) increases with time, approaching a saturation value. The same feature is observed for other w values and other cases (A2 – D2).

The dependence of E_{tr} distribution on the half-period w at a transfer time when the fluctuation is significant (e.g., $t = 1.4$) is shown in Fig. 3. The amplitude of E_{tr} variation over a period, $\Delta E_{tr} = E_{tr}(0) - E_{tr}(w)$ is seen to increase with the half-period w, approaching a limit at large w. This can also be seen from Fig. 4, which shows the time dependence of ΔE_{tr} for various w values. ΔE_{tr} is seen to increase initially to a maximum then decreases to zero in a few 10 units of time t_o.

The corresponding results for other cases are summarized in the next three figures. Figure 5 shows the increase of ΔE_{tr} with w, at a time $t = 10$ (when the fluctuation is still significant), for all cases. The increase is seen to asymptote to the maximum value at $w \geq 10$.
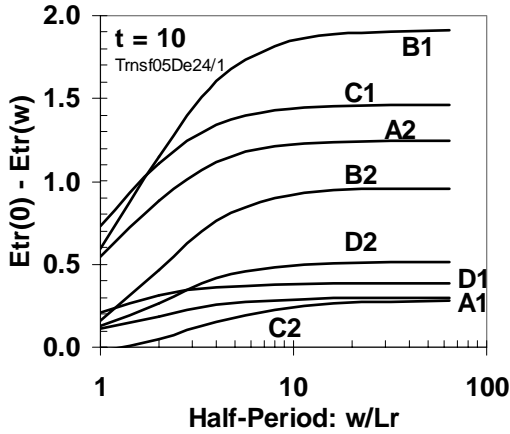
injection become significant. ΔE_{tr} decreases as the transfer time is increased. The same features are seen with other w values.

The time dependence of E_{tr} values averaged over a period of spatial variation for the 8 cases are shown in Fig. 7. In all cases the average E_{tr} increases with time reaching a large asymptotic value after about 100 time units, except the three cases (A2, C2 and D2) with negligible injection $s = 0$. In these latter cases, the asymptotic value is reached at a shorter time, but is significantly lower than that for the other cases, indicating again the importance of charge injection from the electrode in achieving efficient and uniform transfer.
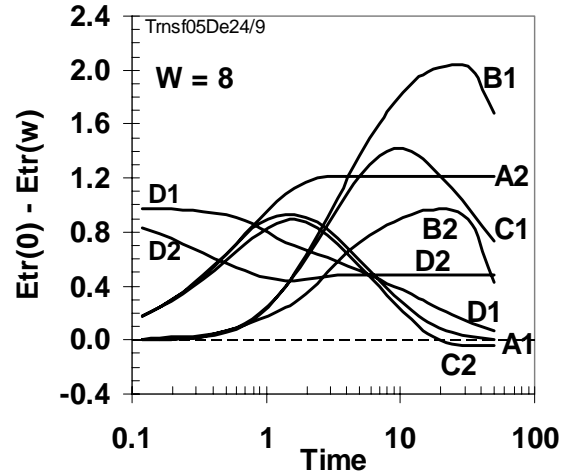

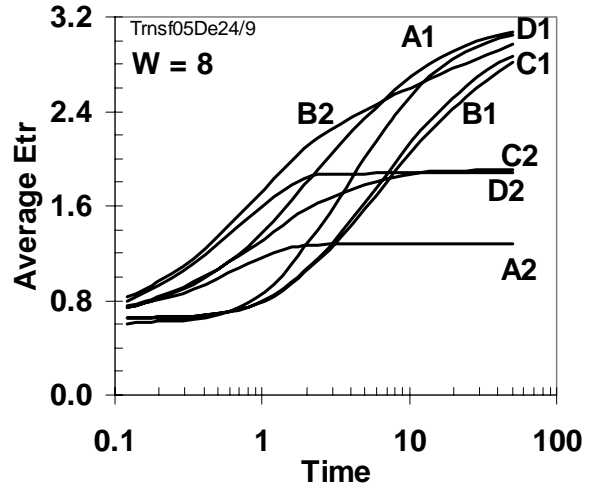**Figure 6.** *Time dependence of ΔE_{tr} for all 8 cases,* represented by examples for half-period $w = 8$.

Figure 5. *Dependence of ΔE_{tr} on half-period w, for all 8 cases, at t = 10.*

Figure 7. *Time dependence of E_{tr} averaged over one period of spatial variation, for all 8 cases, for $w = 8$.*

Figure 6 summarizes the time dependence of ΔE_{tr}, in all 8 cases for $w = 8$. While in many cases ΔE_{tr} decreases to zero at a long time, ($t \geq 100$, as shown in Fig. 4 for Case A1), in Cases A2, C2 and D2, with the injection strength negligibly small ($s = 0$), ΔE_{tr} asymptotes to a finite value even after a long transfer time. This suggests that a significant charge injection from the electrode ($s > 0$) is important in eliminating the E_{tr} variations arising from spatial non-uniformity of the receiver parameters.

In Cases D1 and D2, ΔE_{tr} is large at short time, because the permittivity ε has a large control on E_{tr} before charge transport and

Conclusions

The dielectric relaxation of the receiving media, which is important in efficient transfer of developed toners has been treated by the charge transport model with intrinsic charge density q_i,

charge mobility μ, charge injection strength s and permittivity ε as the transport parameters.[2-4] By representing the spatial variations of these parameters with sinusoidal functions, and considering the variation of each parameter separately, we have obtained the following conclusions.

(1) The fluctuation in transfer field E_{tr} increases with the spatial period 2w of variation in any of the transport parameters, q_i, μ, s, and ε, approaching the asymptotic limit at $w \geq 10$.

(2) The fluctuation in E_{tr} increases with transfer time initially to a maximum, then decreases to a negligible level, provided charge injection from the electrode is significant.

(3) The E_{tr} values averaged over a period increases with time, approaching a large saturation value, unless the charge injection is negligibly small.

The latter two findings combined suggest that the optimum transfer time is of the order of 100 time units t_o. This much time is required to build-up the size of transfer field E_{tr} and "iron-out" the non-uniformity in E_{tr} caused by the non-uniformity in receiver parameters. As the print speed increases, this much time may become unavailable, and hence, the image quality can decline. However, since the time unit t_o (defined in Table II), is determined from the receiver thickness L_r, the charge mobility μ_o and the bias voltage V_b, the actual value of the optimum transfer time can be shortened by reducing the receiver thickness L_r, or increasing the bias voltage V_b and/or the charge mobility μ_o within the ranges of practical applicability.

For typical transfer media, being made of non-homogeneous composite materials, the transport parameters q_i, μ, s, ε can be expected to vary widely with position. The determination of these parameter values for a large number of large area samples is not always practical.[7,8] It is often desired to have a single figure of merit that reveals the effects of all the above transport parameters. For this purpose, we have introduced an "equivalent resistance", which can be determined efficiently over a large area, and under the condition of open-circuit voltage decays as in actual electrostatic transfer process.[6] Examples of the spatial variation of equivalent resistance for a typical intermediate transfer belt, determined by this technique are shown in Ref. 6. The spatial variation discussed in this paper can be deduced from such data.

References

[1] M. C. Zaretsky, J. Imag. Sci. & Tech. **37**, 187 (1993); J. W. May and T. N. Tomb, Proc. IS&T's NIP-13, pg.71 (1997); T. N. Tomb, Proc. IS&T's NIP-14, pg.440 (1998)

[2] I. Chen and M.-K. Tse, Proc. IS&T's NIP-15, pg.155 (1999); M.-K. Tse, D.J. Forest, F.Y. Wang, Proc. IS&T's NIP-15, pg.159 (1999)

[3] I. Chen, Proc. IS&T's NIP-20, pg. 30 (2004)

[4] I. Chen and M.-K. Tse, J. Imag. Sci. & Tech. 44, 462 (2000)

[5] Work similar in objectives but differ in approaches has been reported by N. Provatas, A. Cassidy, & M. Inoue, Proc. IS&T's NIP-20, pg. 958 (2004)

[6] M.-K. Tse and I. Chen, Proc. Japan Hardcopy-2005, pg.199 (2005)

[7] I. Chen and M.-K. Tse, Proc. IS&T's NIP-16, pg. 208 (2000)

[8] I. Chen and M.-K. Tse, Proc. IS&T's NIP-17, pg. 92 (2001)

Author Biography

Inan Chen received his Ph.D. from the University of Michigan in 1964, and worked at Xerox Research Laboratories in Webster, NY, from 1965 to 1998. Currently, he is a consulting scientist for Quality Engineering Associates (QEA), Inc. and others. He specializes in mathematical analyses of physical processes, in particular, those related to electrophotography. He is the recipient of IS&T's 2005 Chester F. Carlson Award. Contact at inanchen@frontiernet.net or www.qea.com.